







## PAPER

[View Article Online](#)  
[View Journal](#) | [View Issue](#)Cite this: *J. Mater. Chem. B*,  
2024, 12, 4717Long-lasting insecticidal activity in plants driven  
by chlorogenic acid-loaded metal–organic  
frameworks†Irene Rincón,<sup>a</sup>  <sup>‡</sup> MCarmen Contreras,<sup>‡</sup> <sup>b</sup> Beatriz Sierra-Serrano,<sup>b</sup>   
Fabrice Salles,<sup>c</sup>  Antonio Rodríguez-Diéguez,<sup>b</sup>  Sara Rojas<sup>b</sup> \*<sup>b</sup> and  
Patricia Horcajada<sup>a</sup> \*<sup>a</sup>

Metal–organic frameworks (MOFs) possess a variety of interesting features related to their composition and structure that make them excellent candidates to be used in agriculture. However, few studies have reported their use as delivery agents of agrochemicals. In this work, the natural polyphenol chlorogenic acid (CGA) was entrapped via simple impregnation in the titanium aminoterephthalate MOF, MIL-125-NH<sub>2</sub>. A combination of experimental and computational techniques was used to understand and quantify the encapsulated CGA in MIL-125-NH<sub>2</sub>. Subsequently, CGA delivery studies were carried out in water at different pHs, showing a fast release of CGA during the first 2 h ( $17.3 \pm 0.3\%$  at pH = 6.5). *In vivo* studies were also performed against larvae of mealworm (*Tenebrio molitor*), evidencing the long-lasting insecticidal activity of CGA@MIL-125-NH<sub>2</sub>. This report demonstrates the potential of MOFs in the efficient release of agrochemicals, and paves the way to their study against *in vivo* models.

Received 23rd October 2023,  
Accepted 13th April 2024

DOI: 10.1039/d3tb02493h

[rsc.li/materials-b](https://rsc.li/materials-b)

## Introduction

Over the last few decades, nanomedicine has allowed us to achieve superior performance in the prevention, diagnosis, and treatment of diseases. Among all the nanocarriers reported so far, metal–organic frameworks (MOFs) have attracted much attention in recent years.<sup>1,2</sup> MOFs are potentially porous crystalline materials based on a regular array of inorganic units connected through organic polycomplexant linkers.<sup>3</sup> They offer multiple versatilities for the accommodation of active ingredients (AIs): adaptable structure based on biocompatible and/or therapeutically active organic ligands and/or cations, large accessible porosity to host a large variety of AIs, and available binding sites where AIs can be anchored.<sup>1</sup>

Following a similar concept, MOFs have recently emerged as agrochemical delivery agents to enhance crop production and quality.<sup>4</sup> This is particularly important since, to keep pace with the increasing demand of the world population, worldwide food production will need to increase by 60% by 2050 (less

than 30 years).<sup>5</sup> Each year, over 3 billion metric tons of crops are produced globally, which require 187 and 4 million metric tons of fertilizers and pesticides, respectively.<sup>6</sup> However, these practices are obsolete as a result of leaching, photodegradation, chemical hydrolysis and microbial decomposition of the applied agrochemicals. In fact, a large proportion of applied agrochemicals (10–75%) do not reach their target,<sup>7,8</sup> and their extensive use results in the contamination of the environment.<sup>9,10</sup> A significant reduction in the needed amount of agrochemicals to assure crop protection could be achieved by MOF-carriers reducing toxicity and increasing their efficacy by: (i) providing combined activities in a single treatment (MOF intrinsic composition and cargo), (ii) protecting the active cargo from degradation, or (iii) controlling the release, keeping active but non-toxic concentrations over long times, and (iv) reducing cost as lower or unique doses will be required. So far, few studies in the literature have reported the potential use of MOFs in agriculture as delivery agents of agrochemicals, such as *cis*-1,3-dichloropropene from Ca-L-lactate MOF,<sup>11</sup> dinotefuran from MIL-101(Fe),<sup>12</sup> azoxystrobin from MIL-100(Fe),<sup>13</sup> tebuconazole from PCN-224,<sup>14</sup> or glufosinate from GR-MOF-7<sup>15</sup> (299 papers, 75% published within the last 3 years, according to Web of Science, March 2024, “agriculture” “metal–organic frameworks”).

With this in mind, we have selected as AI the naturally occurring polyphenol chlorogenic acid (CGA) based on caffeic and quinic acid, with antioxidant, anti-herbivore and fungicidal

<sup>a</sup> Advanced Porous Materials Unit, IMDEA Energy Institute. Av. Ramón de la Sagra 3, 28935 Móstoles-Madrid, Spain. E-mail: [patricia.horcajada@imdea.org](mailto:patricia.horcajada@imdea.org)<sup>b</sup> Department of Inorganic Chemistry, Faculty of Science, University of Granada. Av. Fuentenueva s/n, 18071 Granada, Spain. E-mail: [srojas@ugr.es](mailto:srojas@ugr.es)<sup>c</sup> ICGM, Université Montpellier, CNRS ENSCM, Montpellier, France† Electronic supplementary information (ESI) available. See DOI: <https://doi.org/10.1039/d3tb02493h>

‡ These authors contributed equally to this work.

**Table 1** Textural properties before and after CGA encapsulation and total pesticide loading (wt% and mol mol<sup>-1</sup>) calculated using different techniques

	$S_{\text{BET}}$ (m <sup>2</sup> g <sup>-1</sup> ) $V_p$ (cm <sup>3</sup> g <sup>-1</sup> )		Loaded CGA (wt%, mol mol <sup>-1</sup> )			
	Before encapsulation	After encapsulation	UV-vis	HPLC	EA	TGA
MIL-125-NH <sub>2</sub>	1470 0.50	570 0.19	25.0 ± 6.0 1.18 ± 0.30	29.3 ± 0.8 1.93 ± 0.07	28.9 1.90	27.7 1.80

activity.<sup>16</sup> CGA is a defence metabolite in plants that provides protection against different pathogens, like the pathogenic yeast *Candida albicans*,<sup>17</sup> several phytopathogenic fungi (*Alternaria alternata*, *Sclerotinia sclerotiorum*, *Fusarium solani*, *Verticillium dahliae*, *Botrytis cinerea* and *Cercospora sojina*),<sup>18,19</sup> the tomato fruit worm *Heliothis zea*,<sup>20</sup> leaf beetles *Lochmaea capreae* L.,<sup>21</sup> the tobacco armyworm *Spodoptera litura*,<sup>22</sup> and the western flower thrips *Frankliniella occidentalis*,<sup>23</sup> among others. However, as a natural antioxidant product, its chemical structure is prone to change before or during its application. In particular, CGA has been reported to be very sensitive to pH (between 3 to 10 in soil).<sup>24</sup> In an attempt to improve its stability and activity in the field, CGA has been encapsulated in different polymeric formulations (24 wt% in chitosan nanoparticles,<sup>25</sup> 24 wt% yeast cells,<sup>26</sup> and apple seed protein matrix),<sup>27</sup> but never in a MOF-based material. In this line, we report here the encapsulation and release of CGA in the benchmarked biocompatible highly porous MOF carrier MIL-125-NH<sub>2</sub> (i.e., [Ti<sub>8</sub>O<sub>8</sub>(OH)<sub>4</sub>(BDC-NH<sub>2</sub>)<sub>6</sub>]; BDC-NH<sub>2</sub>: 2-amino-terephthalate, MIL: Material Institute Lavoisier).<sup>28</sup> The selected MOF possesses a variety of interesting features that make it a promising carrier of agrochemicals: i) it is highly porous (Brunauer, Emmett and Teller (BET) surface area of 1400 m<sup>2</sup> g<sup>-1</sup> and pore volume ( $V_p$ ) of 0.6 cm<sup>3</sup> g<sup>-1</sup>), with large cavities (12.5 and 6 Å, accessible *via* windows of ~5–7 Å), compatible with the CGA dimensions (17.0 × 6.1 × 4.9 Å<sup>3</sup>, estimated by Vesta considering van der Waals radii); (ii) it is non-toxic, since after its oral administration (1 g of MIL-125-NH<sub>2</sub> per Kg of rat), this MOF has been demonstrated to be biocompatible and bioeliminable by feces and urine,<sup>29,30</sup> (iii) it can be considered an “active carrier” since MIL-125-NH<sub>2</sub> presents a selective antimicrobial and antibiofilm activity, as recently demonstrated,<sup>31</sup> and it is considered a beneficial element in plant growth, as for example some commercial fertilizers are based on titanium (i.e., Titanit<sup>®</sup>).<sup>32</sup> Thus, we studied in detail the CGA encapsulation in MIL-125-NH<sub>2</sub>, evaluating the efficiency in the release of CGA of the resulting formulation under relevant aqueous solutions at different pHs. Then, the potential antiherbivore activity of the CGA-loaded material was investigated against larvae of *Tenebrio molitor* (mealworm), which is considered a pest in agriculture. To the best of our knowledge, CGA@MIL-125-NH<sub>2</sub> will be the first CGA formulation based on MOFs studied *in vivo*.

## Results and discussion

### CGA encapsulation

The impregnation of the porous material in CGA aqueous solutions led to the successful incorporation of the pesticide. The agrochemical content, estimated by UV-vis spectroscopy,

thermogravimetric analysis (TGA), elemental analysis (EA) and high-performance liquid chromatography coupled with a photodiode array detector (HPLC-PDA), reached *ca.* 30 wt%, corresponding to 1.9 mmol of pesticide per mol of MIL-125-NH<sub>2</sub> (Table 1). Such a value is in very good agreement with the theoretical value (1.85 mmol mol<sup>-1</sup> or 0.2 g g<sup>-1</sup> of dry MIL-125-NH<sub>2</sub>) obtained for saturation by Monte Carlo calculations (see Section S2, ESI<sup>†</sup>). Note that this CGA loading is higher than the previously reported formulations (maximal reported loading 24 wt% of CGA).<sup>25,26</sup> During the incorporation process, the chemical stability of the MOF was confirmed as only 3.8% of the total linker of MIL-125-NH<sub>2</sub> is leached under these conditions. Furthermore, X-ray powder diffraction (XRPD) patterns evidenced that the pesticide incorporation process does not alter the crystalline structure of the porous material (Fig. 1a). Additionally, the absence of Bragg peaks corresponding to the free CGA rules out the presence of free recrystallized pesticide out of the pores. The morphology and water dispersion of CGA@MIL-125-NH<sub>2</sub> were characterized by field emission scanning electron microscopy (FE-SEM) and dynamic light scattering (DLS), respectively. No differences between the shape and size of the cubic MIL-125-NH<sub>2</sub> nanoparticles are observed after the CGA loading (Fig. 1c and d). Furthermore, CGA@MIL-125-NH<sub>2</sub> water solution exhibited larger particle sizes, between 226 ± 83 to 653 ± 97 nm (ESI<sup>†</sup>, Fig. S6), similar to previously reported MIL-125-NH<sub>2</sub>.<sup>33,34</sup>

The incorporation of CGA into the cavities of MIL-125-NH<sub>2</sub> was demonstrated by the reduction of the N<sub>2</sub> sorption capacity of the MOF (Fig. 1b). In particular, CGA@MIL-125-NH<sub>2</sub> keeps a significant residual porosity (570 m<sup>2</sup> g<sup>-1</sup>). This decrease in accessible porosity is confirmed by theoretical calculations performed on the CGA-saturated structure for which the specific surface area and the pore volume evolve from 1900 to 1275 m<sup>2</sup> g<sup>-1</sup> and 0.77 to 0.67 cm<sup>3</sup> g<sup>-1</sup>, respectively. The dimensions of CGA (17.0 × 6.1 × 4.9 Å<sup>3</sup>) are compatible with its encapsulation in MIL-125-NH<sub>2</sub> particularly into the micropores of MIL-125-NH<sub>2</sub> (accessible *via* ~5–7 Å windows). In this regard, to shed some light on the influence of porosity on CGA encapsulation, the potentially maximum CGA adsorption capacity was estimated by taking into account the pore volume of MIL-125-NH<sub>2</sub> and the theoretical volume of CGA. Accordingly, 20% of the theoretical maximum CGA loading (2.5 mol of CGA per mol of MIL-125-NH<sub>2</sub>) should be located in the tetrahedral void. Considering that we achieved a maximum 1.9 mmol of CGA loading, we can suggest the absence of any encapsulation within the smaller cages of MIL-125-NH<sub>2</sub>. This could be related to the interaction of the hydrophilic and hydrogen bond acceptor –NH<sub>2</sub> group in the organic linker with water





**Fig. 1** (a) XRPD patterns of pristine and CGA loaded MIL-125-NH<sub>2</sub>. Free CGA XRPD pattern was added for comparison. (b) N<sub>2</sub> sorption isotherms (77 K) for MIL-125-NH<sub>2</sub> before (black, circles), and after (red, squares) the CGA loading. Empty symbols denote desorption. FE-SEM images of (c) MIL-125-NH<sub>2</sub> and (d) CGA@MIL-125-NH<sub>2</sub>. No significant differences after the CGA encapsulation are observed in the cubic shaped particles.

molecules. Considering the CGA as rigid, Monte Carlo simulations show that the CGA molecule can only enter in the structure in the largest pores (see Fig. 2a illustrating the density of presence of the molecules). This preferential interaction tends to block the accessibility of the smaller cages as previously observed in the adsorption of caffeine.<sup>35</sup>

Fourier transform infrared (FTIR) spectroscopic analysis shows the presence of the main band of pure CGA (1690 cm<sup>-1</sup>) in the IR spectrum of CGA@MIL-125-NH<sub>2</sub> (ESI†, Fig. S7). Furthermore, the IR spectrum of CGA@MIL-125-NH<sub>2</sub> confirmed a wavelength shift in comparison with the bare MIL-125-NH<sub>2</sub> (from 1541 to 1529 cm<sup>-1</sup> (N–H deformation) for

MIL-125-NH<sub>2</sub> and CGA@MIL-125-NH<sub>2</sub>, respectively). One could tentatively propose the formation of hydrogen bonds between the carboxylic and hydroxyl groups in the CGA with the NH<sub>2</sub> groups present within the MOF. As illustrated in Fig. 2b, strong interactions between both carboxylates and OH groups from CGA were equally found with the NH<sub>2</sub> groups from the MOF structure. Indeed, in Fig. 2b, the distances between the OH and NH<sub>2</sub> groups were close to 2.7 Å, while carboxylate groups interact with 3.2 Å distances with NH<sub>2</sub> groups. One could also consider the deprotonated form of CGA during the encapsulation in aqueous solution (pH = 6.5 and 8; pK<sub>a</sub> = 3.3).<sup>36</sup> However, the same interactions were observed, OH groups from the





Fig. 2 (a) Density of presence for the CGA (green dots) in MIL-125-NH<sub>2</sub> obtained from GCMC simulations, (b) snapshots illustrating the main interactions between the neutral CGA and the MOF, and (c) snapshots illustrating the main interactions between the ionic CGA (compensated by Na<sup>+</sup>) and the MOF. The colours of the atoms are the following: H (white), C (black), O (red), N (blue) and Ti (grey).

anionic CGA interacting with the NH<sub>2</sub> groups from the MOF (distances close to 2.7–2.9 Å; Fig. 2c).

### CGA delivery

In order to envisage the potential applications as a CGA controlled delivery system, the CGA-release properties of CGA@MIL-125-NH<sub>2</sub> were tested in aqueous media by HPLC (see ESI,† Section S3 for experimental details). Note that water was selected as typically agrochemicals are sprayed as aqueous solutions or suspensions and will be delivered by the plant or soil humidity/rain effect.<sup>37</sup> First, as CGA was reported to be very sensitive to pH,<sup>24</sup> the stability of CGA and its release in water at different pH values (pH = 4, 6.5 and 8) were assessed. Free CGA remains stable at pH 4 and 6.5, but an important degradation is observed at pH 8 (with less than 10% of the initial CGA after

7 days; Fig. S8, ESI†). From the CGA@MIL-125-NH<sub>2</sub>, a fast release of CGA occurs during the first 2 h in all studied media (34.5 ± 1.8, 17.3 ± 0.3, and 46.8 ± 2.6% at pH 4, 6.5 and 8, respectively; Fig. 3). Then, a slower and partial release of CGA is observed. When comparing the CGA delivery in the different media, one can observe the relation between the CGA release and the MOF stability (linker release), the latter increasing from pH = 8 < pH = 4 < 6 pH = 6.5. It should be noted that along all the experiment (7 days) the concentration of CGA remains stable in all tested media, which demonstrates the utility of MIL-125-NH<sub>2</sub> in the controlled release of CGA and its protective effect (specially at pH = 8). This slow and sustained CGA release may be due to the slow diffusion of CGA through the MIL-125-NH<sub>2</sub> windows (~5–7 Å, connecting the cages), with a similar size to the CGA dimensions (17.0 × 6.1 × 4.9 Å<sup>3</sup>) and to the



Fig. 3 CGA release (black squares) from CGA@MIL-125-NH<sub>2</sub> and leached linker (H<sub>2</sub>BDC-NH<sub>2</sub>, red circles) in aqueous media at different pHs (4, 6.5, and 8 from left to right) during (a) 168 h (7 days), and (b) 10 h.





formation of specific CGA–MOF interactions (Fig. 2; see above). Note here that the remaining amount of CGA in MIL-125-NH<sub>2</sub> after 7 days of release was confirmed by TGA (*ca.* 72% at pH 6.5).

On the other hand, to assess temporal stability, the CGA@MIL-125-NH<sub>2</sub> sample was stored at room temperature, without any special requirements. After 3 months, the CGA@MIL-125-NH<sub>2</sub> material remains crystalline, as demonstrated by its XRPD pattern (ESI,† Fig. S9).

Aside from CGA release as an insecticide, one should consider the advantageous effect of the release of Ti associated with the matrix degradation. Ti is considered a beneficial element in plant growth. Several commercial fertilizers containing Ti (*i.e.*, Tytanit and Mg-Titanit) have been used as biostimulants for improving crop production.<sup>32</sup> In this regard, the potential growth effect of MIL-125-NH<sub>2</sub> was tested in *Lolium multiflorum* (annual ryegrass) seeds, used here as a model plant (ESI,† Fig. S11). Seeds were grown in aqueous suspensions of MIL-125-NH<sub>2</sub> with different concentrations (from 50 to 750 ppm) or in water (used as control), and the length of the stem and roots, and dried weight of the plants were measured after 7 days. At the studied concentrations, no significant differences (*p*-value < 0.05) were found between groups under the tested conditions. Thus, it can be concluded that non-biostimulant nor toxic effects in plant growth can be associated with MIL-125-NH<sub>2</sub>. Furthermore, according to the MOF degradation in water (2.9% after 2 h), the total Ti concentration after 2 h is 0.59 mg mL<sup>-1</sup>. Thus, considering the Pourbaix diagram of Ti at the working pH (pH = 6), Ti should be as TiO<sub>2</sub>, considered a safe metal oxide which does not exhibit acute toxicity to soil earthworms.<sup>38</sup>

Finally, the CGA release kinetics was fitted to a mathematical model in order to better understand the potentially involved mechanism. In particular, the Higuchi model (ESI,† Section S5), which defines the short time behaviour of the release of a dispersed cargo from a matrix has been used to

describe the diffusion of the CGA from the MOF.<sup>39</sup> This model, normally used to describe the release of drugs, perfectly describes release processes where the cargo is dispersed in stable monolithic systems (with no changes during the release process), with the release being purely controlled by diffusion. As previously described in the drug release from biodegradable matrices,<sup>40</sup> Higuchi's equation is verified at early times, avoiding an important degradation of the material where this model would not fit.

### Insecticidal activity assay

To demonstrate the applicability of the CGA-loaded MIL-125-NH<sub>2</sub> in agriculture, the potential insecticidal activity of CGA@MIL-125-NH<sub>2</sub> against the larvae of mealworms (*Tenebrio molitor*) was tested, and compared with the free CGA and pristine MOF as controls. Previous to any test, the active CGA concentration against larvae of *T. molitor* was determined (200 mg of CGA per gram of oat), considering previous reports on the activity of CGA against different herbivores.<sup>41</sup> Then, larvae were fed with repeated doses of oats (1 g) previously doped with an aqueous suspension of CGA (200 mg), MIL-125-NH<sub>2</sub> (441.2 mg), or CGA@MIL-125-NH<sub>2</sub> (683.2 mg). Note that the administered quantity of each group was adjusted to the corresponding part of CGA or MIL-125-NH<sub>2</sub> (see further details in ESI,† Section S7). The Probit analysis was used to calculate the median lethal time (LT<sub>50</sub>) to compare the isolates effectiveness.<sup>42</sup> When *T. molitor* was fed with CGA-containing oat, 97.5% of larvae died after 21 days of the first treatment (Fig. 4), which corresponds to a LT<sub>50</sub> of 7.5 days.

After 21 days, CGA@MIL-125-NH<sub>2</sub> is significantly (*p* < 0.05) more active (92.5 ± 3.5% of mortality) than pristine MIL-125-NH<sub>2</sub> (72.5 ± 3.5% of mortality), with an LT<sub>50</sub> of 16.1 and 17.3 days respectively. On the other hand, when treated with pristine MIL-125-NH<sub>2</sub> and CGA@MIL-125-NH<sub>2</sub> for 21 days, a



Fig. 4 Images of larvae of *T. molitor* sprayed with CGA@MIL-125-NH<sub>2</sub> and water (control), and (b) insecticidal effect after 21 days of the first administration of oat, CGA, MIL-125-NH<sub>2</sub>, and CGA@MIL-125-NH<sub>2</sub> to larvae of *T. molitor*.



progressive larvae mortality was evidenced (ESI,† Fig. S12). As expected, the pristine CGA has a faster effect on larvae death than the CGA-loaded MOF, but as mentioned during the introduction the use of high doses of agrochemicals could lead to toxic effects in the environment. These results are indicative of the enhanced long-lasting insecticidal activity of CGA@MIL-125-NH<sub>2</sub> related with the progressive release of the CGA, and therefore, associated with a reduced environmental toxicity.

## Conclusions

A new agrochemical formulation based on a highly porous MOF and chlorogenic acid (CGA), with antioxidant, anti-herbivore and fungicidal activity, is here presented as an attractive formulation to improve pesticide activity, while decreasing environmental toxicity. The CGA was easily encapsulated into MIL-125-NH<sub>2</sub> (water suspension for 24 h) surpassing the loading achieved using other CGA formulations. Furthermore, the CGA release was fast (17.3% in 2 h), retaining 72% of CGA in MIL-125-NH<sub>2</sub> after 7 days. Upon the treatment of *T. molitor* (a pest in agriculture) with oats supplemented with CGA@MIL-125-NH<sub>2</sub>, a progressive toxic effect was observed and associated with a reduced environmental toxicity. These results pave the way to efficiently delivering potentially toxic agrochemicals via a convenient porous formulation, avoiding toxic effects associated with high concentrations of agrochemicals in our fields.

## Conflicts of interest

There are no conflicts to declare.

## Acknowledgements

This research publication has been funded by the project MOFseidon PID2019-104228RB-I00, AgroMOFs TED2021-132440B-I00 and MOFCycle CNS2022-135779 funded by MCIN/AEI/10.13039/501100011033, B-FQM-394, and ProyExcel\_00105 funded by Junta de Andalucía. S.R. is grateful for the grant (RYC2021-032522-I) funded by MCIN/AEI/10.13039/501100011033 and for El FSE invierte en tu futuro. Funding for open access charge: University of Granada/CBUA.

## References

- 1 S. Rojas, A. Arenas-Vivo and P. Horcajada, *Coord. Chem. Rev.*, 2019, **388**, 22–226.
- 2 M. Giménez-Marqués, T. Hidalgo, C. Serre and P. Horcajada, *Coord. Chem. Rev.*, 2015, **307**, 342–360.
- 3 H. C. J. Zhou and S. Kitagawa, *Chem. Soc. Rev.*, 2014, **43**, 5415–5418.
- 4 S. Rojas, A. Rodríguez-Diéguez and P. Horcajada, *ACS Appl. Mater. Interfaces*, 2022, **14**, 16983–17007.
- 5 United Nations, *Revision of World Population Prospects*, 2019.
- 6 G. V. Lowry, A. Avellan and L. M. Gilbertson, *Nat. Nanotechnol.*, 2019, **14**, 517–522.
- 7 W. Aktar, D. Sengupta and A. Chowdhury, *Interdiscip. Toxicol.*, 2009, **2**, 1–12.
- 8 D. Pimentel, *Environ. Dev. Sustainable*, 2005, **7**, 229–252.
- 9 L. Comoretto, B. Arfib and S. Chiron, *Sci. Total Environ.*, 2007, **380**, 124–132.
- 10 C. Sun, *Development and Efficacy Evaluation of Novel Adhesive Pesticide Nano-Delivery Systems*, University of Liege, 2019.
- 11 J. Yang, C. A. Trickett, S. B. Alahmadi, A. S. Alshammari and O. M. Yaghi, *J. Am. Chem. Soc.*, 2017, **139**, 8118–8121.
- 12 P. Feng, J. Chen, C. Fan, G. Huang, Y. Yu, J. Wu and B. Lin, *J. Cleaner Prod.*, 2020, **265**, 121851.
- 13 Y. Shan, L. Cao, B. Muhammad, B. Xu, P. Zhao, C. Cao and Q. Huang, *J. Colloid Interface Sci.*, 2020, **566**, 383–393.
- 14 J. Tang, G. Ding, J. Niu, W. Zhang, G. Tang, Y. Liang, C. Fan, H. Dong, J. Yang, J. Li and Y. Cao, *Chem. Eng. J.*, 2019, **359**, 225–232.
- 15 B. Sierra-Serrano, A. García-García, T. Hidalgo, D. Ruiz-Camino, A. Rodríguez-Diéguez, G. Amariei, R. Rosal, P. Horcajada and S. Rojas, *ACS Appl. Mater. Interfaces*, 2022, **14**, 34955–34962.
- 16 A. Kundu and J. Vadassery, *Plant Biol.*, 2019, **21**, 185–189.
- 17 W. S. Sung and D. G. Lee, *Pure Appl. Chem.*, 2010, **82**, 219–226.
- 18 E. Wojciechowska, C. H. Weinert, B. Egert, B. Trierweiler, M. Schmidt-Heydt, B. Horneburg, S. Graeff-Hönniger, S. E. Kulling and R. Geisen, *Eur. J. Plant Pathol.*, 2014, **139**, 735–747.
- 19 G. Martínez, M. Regente, S. Jacobi, M. Del Rio, M. Pinedo and L. de la Canal, *Pestic. Biochem. Physiol.*, 2017, **140**, 30–35.
- 20 C. A. Elliger, Y. Wong, B. G. Chan and A. C. Waiss, *J. Chem. Ecol.*, 1981, **7**, 753–758.
- 21 A. Ikonen, J. Tahvanainen and H. Roininen, *Entomol. Exp. Appl.*, 2001, **99**, 47–54.
- 22 N. Mallikarjuna, K. R. Kranthi, D. R. Jadhav, S. Kranthi and S. Chandra, *J. Appl. Entomol.*, 2004, **128**, 321–328.
- 23 K. A. Leiss, F. Maltese, Y. H. Choi, R. Verpoorte and P. G. L. Klinkhamer, *Plant Physiol.*, 2009, **150**, 1567–1575.
- 24 J. Dow, *J. Exp. Biol.*, 1992, **172**, 355–375.
- 25 B. Niu, H. Chen, W. Wu, X. Fang, H. Mu, Y. Han and H. Gao, *Food Chem.: X*, 2022, **14**, 100312.
- 26 G. Shi, L. Rao, H. Yu, H. Xiang, G. Pen, S. Long and C. Yang, *J. Food Eng.*, 2007, **80**, 1060–1067.
- 27 A. Gani, Z. U. Ashraf, A. Shah, A. S. Naik, I. A. Wani and A. Gani, *Foods*, 2022, **11**, DOI: [10.3390/foods11223702](https://doi.org/10.3390/foods11223702).
- 28 M. Dan-Hardi, C. Serre, T. Frot, L. Rozes, G. Maurin, C. Sanchez and G. Férey, *J. Am. Chem. Soc. Commun.*, 2009, **131**, 10857–10859.
- 29 S. Rojas, N. Guillou and P. Horcajada, *ACS Appl. Mater. Interfaces*, 2019, **11**, 22188–22193.
- 30 T. Baati, L. Njim, F. Neffati, A. Kerkeni, M. Bouttemi, R. Gref, M. F. Najjar, A. Zakhama, P. Couvreur, C. Serre and P. Horcajada, *Chem. Sci.*, 2013, **4**, 1597–1607.



- 31 Z. A. Khan, E. S. Goda, A. Ur Rehman and M. Sohail, *Mater. Sci. Eng., B*, 2021, **269**, 115146.
- 32 S. Lyu, X. Wei, J. Chen, C. Wang, X. Wang and D. Pan, *Front Plant Sci.*, 2017, **8**, DOI: [10.3389/fpls.2017.00597](https://doi.org/10.3389/fpls.2017.00597).
- 33 S. M. F. Vilela, P. Salcedo-Abraira, I. Colinet, F. Salles, M. C. De Koning, M. J. A. Joosen, C. Serre and P. Horcajada, *Nanomaterials*, 2017, **7**, 321–336.
- 34 A. Arenas-Vivo, S. Rojas, I. Ocaña, A. Torres, M. Liras, F. Salles, D. A. Esteban, S. Bals, D. Avila Brande and P. Horcajada, *J. Mater. Chem. A*, 2021, **9**, 15704–15713.
- 35 D. Cunha, C. Gaudin, I. Colinet, P. Horcajada, G. Maurin and C. Serre, *J. Mater. Chem. B*, 2013, **1**, 1101–1108.
- 36 “DrugBank,” 2024.
- 37 T. Tadros, in *Encyclopedia of Colloid and Interface Science*, ed. T. Tharwat, Springer, Wokingham, 2013, pp. 3–80.
- 38 J. E. Cañas, B. Qi, S. Li, J. D. Maul, S. B. Cox, S. Das and M. J. Green, *J. Environ. Monit.*, 2011, **13**, 3351–3357.
- 39 T. Higuchi, *J. Pharm. Sci.*, 1963, **52**, 1145–1149.
- 40 A. Charlier, B. Leclerc and G. Couarraze, *Release of Mifepristone from Biodegradable Matrices: Experimental and Theoretical Evaluations*, 2000.
- 41 A. Kundu, S. Mishra and J. Vadassery, *Planta*, 2018, **248**, 981–997.
- 42 D. J. Finney, *Probit Analysis: A Statistical Treatment of the Sigmoid Response Curve*, University Of Oxford, London, Cambridge, 1971.

